

Electronic Supporting Information for:

A Chiral 3D Silver(I)-Benzenedithiolate Coordination Polymer exhibiting Photoemission and Non Linear Optical Response

Saly Hawila,^a Ahmad Abdallah,^a Jean-Luc Rukemampunzi,^a Alexandra Fateeva,^b
Gilles Ledoux,^c Régis Debord,^c Stéphane Pahlès,^c Nathalie Guillou,^d Florian
Massuyeau,^e Romain Gautier,^e Adel Mesbah^a and Aude Demessence^{*a,f}

- a. Université Lyon, Université Claude Bernard Lyon 1, Institut de Recherches sur la Catalyse et l'Environnement de Lyon (IRCELYON), UMR CNRS 5256, Villeurbanne, France.
- b. Université Lyon, Université Claude Bernard Lyon 1, Laboratoire des Multimatériaux et Interfaces (LMI), UMR CNRS 5615, Villeurbanne, France.
- c. Université Lyon, Université Claude Bernard Lyon 1, Institut Lumière Matière (ILM), UMR CNRS 5306, Villeurbanne, France.
- d. Université Paris-Saclay, UVSQ, Institut Lavoisier de Versailles (ILV), UMR CNRS 8180, Versailles, France.
- e. Nantes Université, CNRS, Institut des Matériaux de Nantes Jean Rouxel (IMN), Nantes, France.
- f. BCMaterials (Basque Center for Materials, Applications & Nanostructures), University of the Basque Country (UPV/EHU), Leioa, Spain.

e-mail: aude.demessence@ircelyon.univ-lyon1.fr

Chem. Commun.

Experimental and Instrumentation

Chemicals and materials. Silver nitrate (AgNO_3 , $\geq 99.0\%$), 1,3-Benzenedithiol, 99 %, and 1.0 M lithium triethylborohydride in THF were purchased from Sigma Aldrich. Ethanol and DMF were purchased from VWR Chemicals. All reagents and solvents were used as received.

Synthesis of $[\text{Ag}_2(1,3\text{-BDT})]_n$. An argon flow was bubbled in a solution of AgNO_3 (200 mg, 1.18 mmol, 2 eq.) in water (10 mL) for 5 min. Then 1,3-Benzenedithiol (69 μL , 0.60 mmol, 1 eq.) was added and the reaction was allowed to proceed for 2 h at 120 °C in a 20 ml sealed vial. The white-off precipitate was recovered by centrifugation at 4000 rpm and washed three times with DMF and three times with ethanol. Yield: 59 % (125 mg). Chemical Formula: $\text{C}_6\text{H}_4\text{Ag}_2\text{S}_2$. Molecular Weight: 355.96. Silver content from TGA (calc.) wt%: 60.2 (60.6). Elemental analysis: (calc.) wt%: S 18.63 (18.02), H 1.04 (1.13), C 20.80 (20.25).

Attempts of reduction of $[\text{Ag}_2(1,3\text{-BDT})]_n$. Powder of $[\text{Ag}_2(1,3\text{-BDT})]_n$ is dispersed in a solution of 1.0 M lithium triethylborohydride (LiEt_3BH) in THF for 5 and 20 min and then washed with water, THF and ethanol. The powder remains yellow after 5 min and turns green after 20 min. From PXRD no decomposition is observed and $[\text{Ag}_2(1,3\text{-BDT})]_n$ is still highly crystalline in both cases (Fig. S19).

Characterization techniques.

Routine PXRD. Routine powder X-ray diffraction was carried out on a Bruker D8 Advance A25 diffractometer using $\text{Cu K}\alpha$ radiation equipped with a 1-dimensional position-sensitive detector (Bruker LynxEye). XR scattering was recorded between 4° and 90° (2θ) with 0.02° steps and 0.5 s per step (28 min for the scan). Divergence slit was fixed to 0.2° and the detector aperture to 189 channels (2.9°).

FTIR. The infrared spectra were obtained from a Bruker Vector 22 FT-IR spectrometer with KBr pellets at room temperature and registered from 4000 cm^{-1} to 400 cm^{-1} .

TGA. Thermo-gravimetric analyses (TGA) were performed with a TGA/DSC 1 STARe System from Mettler Toledo. Around 2 mg of sample was heated at a rate of 10 °C.min⁻¹, in a 70 μL alumina crucible, under air atmosphere (20 mL.min⁻¹).

UV-vis. UV-vis absorption spectrum was carried out with a LAMBDA 365 UV/Vis Spectrophotometer from Perkin Elmer in solid state with KBr at room temperature.

SEM. SEM images were obtained with FEI Quanta 250 FEG scanning electron microscope. Samples were mounted on stainless pads and sputtered with carbon to prevent charging during observation. A back-scattered electron detector was used to get a better contrast on the calcined samples to observe the presence of β -Ag₂S and Ag.

TEM. Transmission electron microscopy was carried out on a JEOL 2010 LaB₆ microscope operating at 200 kV. Samples were prepared on a copper grid for analysis.

Structure resolution. High-resolution X-ray powder diffraction data were collected on the CRISTAL beamline at Soleil Synchrotron (Gif-sur-Yvette, France). A monochromatic beam was extracted from the U20 undulator beam by means of a Si(111) double monochromator. Its wavelength of 0.67122 Å was refined from a LaB₆ (NIST Standard Reference Material 660a) powder diagram recorded prior to the experiment. The sample was loaded in a 0.7 mm capillary (Borokapillaren, GLAS, Schönwalde, Germany) mounted on a spinner rotating at about 5 Hz to improve the particles' statistics. Diffraction data were collected in continuous scanning mode with a MYTHEN2 X 9K detector (Dectris) allowing a measurement in less than 5 minutes.

Calculations of structural investigations were performed with the TOPAS (indexing, charge flipping, simulated annealing, difference Fourier calculations, Rietveld refinement), EXPO (direct methods) and FOX (simulated annealing) programs.¹ The LSI-indexing method converged unambiguously to a cubic unit cell with satisfactory figures of Merit (see Table S1). Synchrotron data revealed that systematic extinctions were consistent with the $P2_13$ space group (instead of $P4_132$ previously suggested from laboratory data), which was used to initialize the structural determination. Among the solutions obtained by the different programs, the simulated annealing process of FOX software, allowed location of the organic ligand in general position and three independent Ag⁺ cations, one in general position and two others on the threefold axis. The remaining Ag⁺ cation was localized by difference Fourier map calculations. The final Rietveld plot (Fig. S4), for which the phenyl group was treated as rigid body, corresponds to satisfactory model indicator and profile factors (see Table S1). This

involved the following structural parameters: 1 scale factor, 12 atomic coordinates for Ag and S atoms, 6 parameters for the orientation and the translation of the phenyl ring, 1 distance and 3 temperature factors.

CCDC-2164441 contains the supplementary crystallographic data.

***In situ* PXRD experiments with temperature.** High-resolution X-ray powder diffraction data were collected on the CRISTAL beamline at Soleil Synchrotron (Gif-sur-Yvette, France). *In situ* PXRD experiments were performed using the same setup and the wavelength mentioned above. The capillary was left open and the temperature was raised using a heat blower. The sample is heated to 500°C at 10°C.min⁻¹, and then cooled at the same rate by turning off the blower. Phase quantification of each phase was conducted using the fullprof_suite program.

Formation of pellets and density measurements. A mechanical press is used for the formation of pellets for conductivity experiments. Between 40-50 mg of crushed powder sample is introduced in a sample chamber. Then a pressure of 700 MPa or 1 GPa is applied for 15 minutes. The diameter of the pellets is 4 mm and the thickness between 1 and 1.5 mm. The density of the pellets is measured by using the Archimedes' principle in absolute ethanol.

Electrical properties using the four point probe method. The electrical resistivity is measured by means of a Keithley 2450 sourcemeter instrument associated with a linear array of four probes (Jandel). The four probes are made of tungsten carbide (300 µm in diameter) and have a 500 µm spacing. [The applied force on the probes was controlled and monitored around 60 g via a force gauge placed under the sample holder.]. I-V measurements were recorded from which the resistance (R) was extracted by using a linear fit in the range where it behaves linearly.

The conductivity (ρ) is obtained from this equation :

$$\rho = R * 2\pi * S$$

with R, the resistance obtained from the Ohm's law and S, the distance between the electrodes (S = 600 µm).

Photoluminescence excitation and emission spectra measurements. The photoluminescence measurements were performed on a homemade apparatus at Institut

Lumière Matière, University of Lyon. The sample was illuminated by an EQ99X laser driven light source filtered by a Jobin Yvon Gemini 180 monochromator. The exit slit from the monochromator was then reimaged on the sample by two 100m focal length, 2 inch diameter MgF₂ lenses. The whole apparatus has been calibrated by means of a Newport 918D Low power calibrated photodiode sensor over the range 190-1000 nm. The resolution of the system being 4 nm. The emitted light from the sample is collected by an optical fiber connected to a Jobin-Yvon TRIAX320 monochromator equipped with a cooled CCD detector. At the entrance of the monochromator different long pass filter can be chosen in order to eliminate the excitation light. The resolution of the detection system is 2 nm. Temperature control over the sample was regulated with a THMS-600 heating stage with T95-PE temperature controller from Linkam Scientific Instruments.

SHG signal. A Ti:Sa laser from Spectra Physics (Hurricane model) delivering pulse of 100 fs at 800 nm (1 kHz) was used to detect SHG signals. SHG was collected at 400 nm with a streak camera C7700 from Hamamatsu coupled with a spectrometer from Princeton instrument. Potassium dihydrogenphosphate (KDP) as a pellet is first measured as a reference. Then one experiment is done on the powder of [Ag₂(1,3-BDT)]_n with the same conditions as KDP and with more gain to enhance the detected signal.

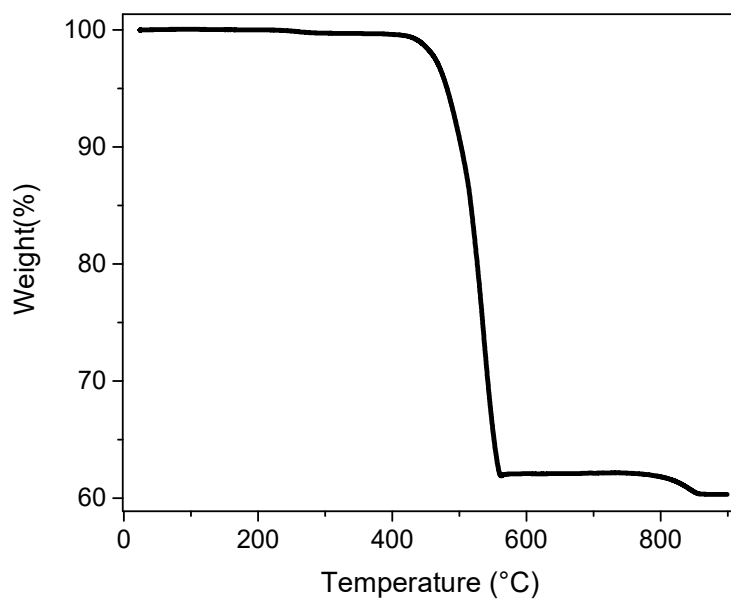


Figure S1. TGA of $[\text{Ag}_2(1,3\text{-BDT})]_n$ carried out under air at $10\text{ }^\circ\text{C}/\text{min}$. The remained silver content at 900°C is 60.2 %.

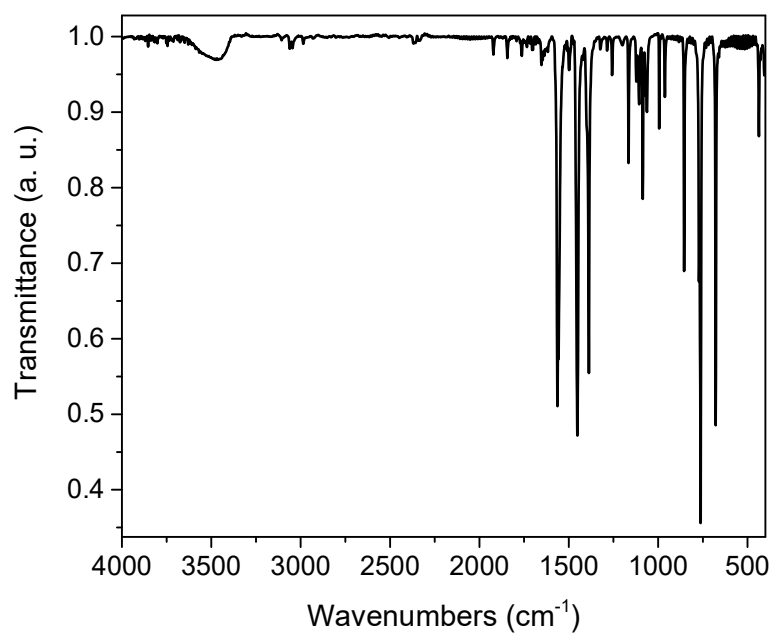


Figure S2. FT-IR spectrum of $[\text{Ag}_2(1,3\text{-BDT})]_n$.

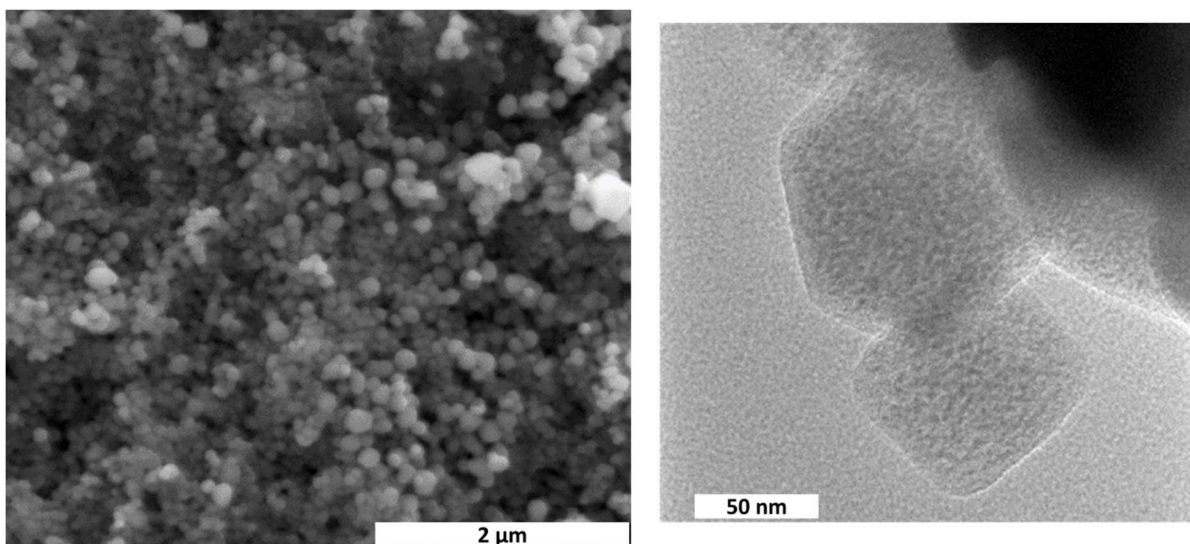


Figure S3. SEM (left) and TEM (right) images of $[\text{Ag}_2(1,3\text{-BDT})]_n$.

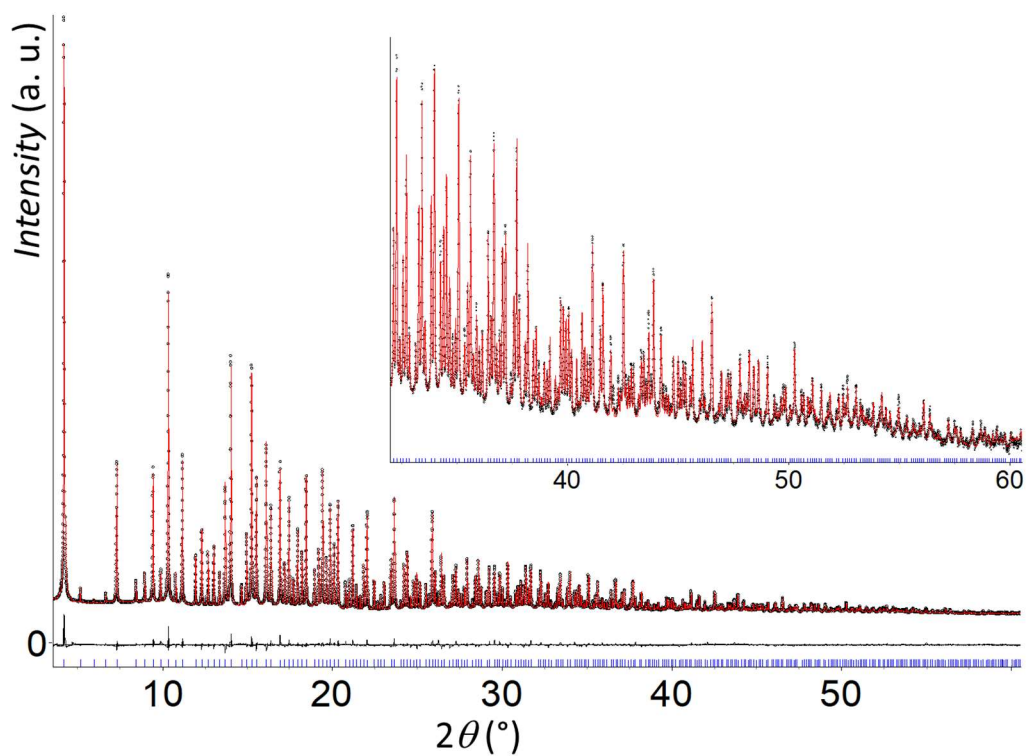


Figure S4. Final Rietveld plot of $[\text{Ag}_2(1,3\text{-BDT})]_n$ showing observed (black dots), calculated (red line), and difference (black line) curves ($\lambda = 0.67122 \text{ \AA}$). A zoom is shown as inset.

Table S1. Crystallographic data and Rietveld refinement parameters for $[\text{Ag}_2(1,3\text{-BDT})]_n$.

Compound	$[\text{Ag}_2(1,3\text{-BDT})]_n$
Empirical formula	$\text{C}_6 \text{H}_5 \text{Ag}_2 \text{S}_2$
M_r	355.96
Crystal system	Cubic
Space group	$P 2_1 3$
a (Å)	12.88562(3)
V (Å ³)	2139.52(2)
M_{20}	567
Z	12
λ (Å)	0.67122
No of structural	23
Number of reflections	1448
R_p, R_{wp}	0.0341, 0.0343
$R_{\text{Bragg}}, \text{GoF}$	0.0371, 3.82

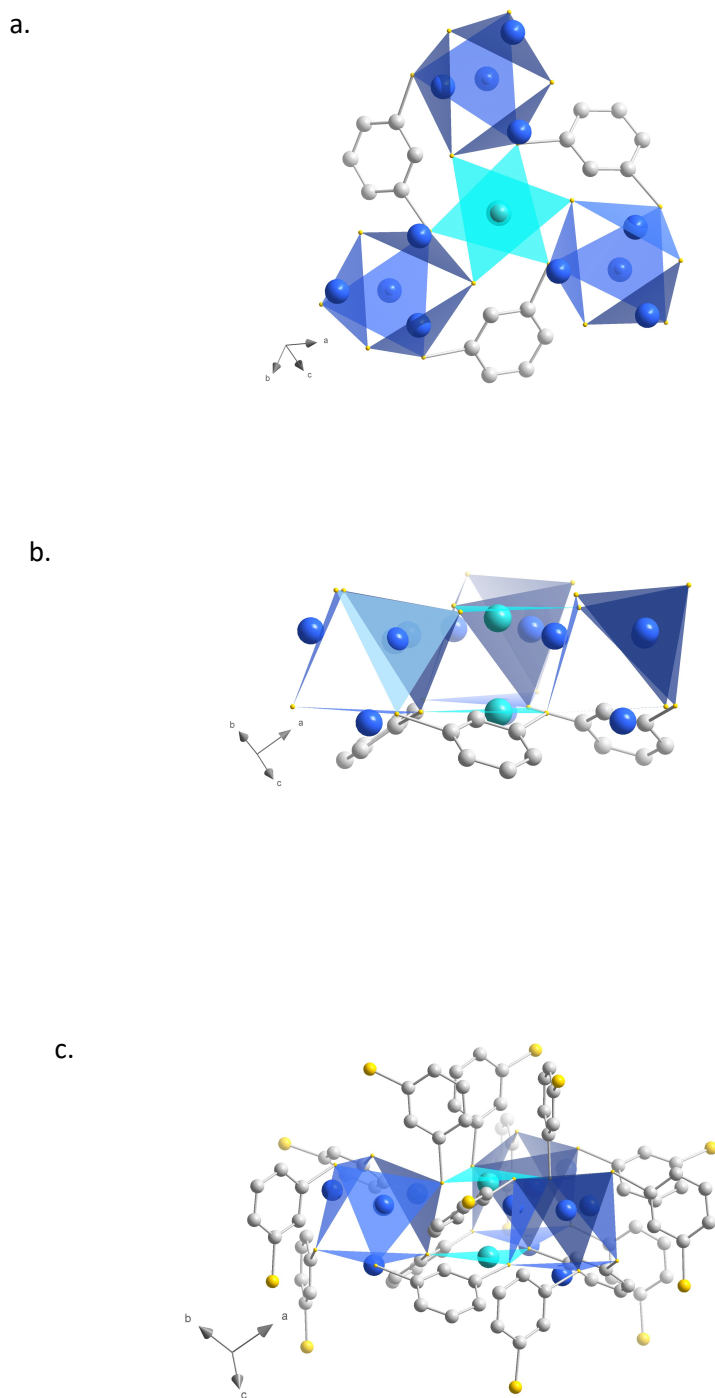


Figure S5. Views of the Ag_2S_6 octahedron (in cyan) connected to three Ag_4S_6 octahedra (in blue) in $[\text{Ag}_2(1,3\text{-BDT})]_n$: a. with the three bridging 1,3-benzenedithiolate ligands, b. same as a. with 90° rotation and c. similar to b. with the additional twelve non-bridging (to this 14-Ag motif) 1,3-benzenedithiolate ligands. Blue, cyan, yellow and grey spheres are for Ag1 and Ag3, Ag2 and Ag4, sulfur and carbon atoms, respectively. Hydrogen atoms have been omitted for clarity.

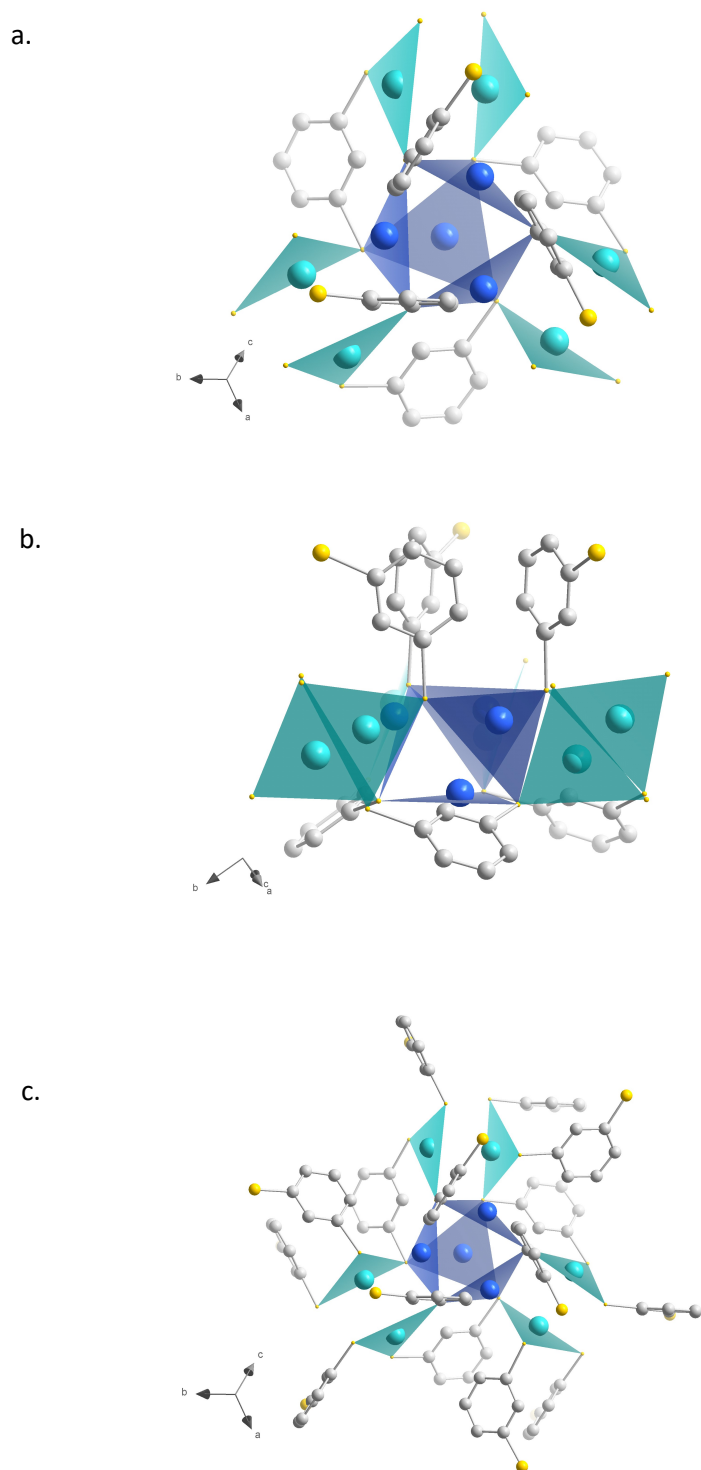


Figure S6. Views of Ag_4S_6 octahedron (in blue) connected to three Ag_2S_6 octahedron (in cyan) in $[\text{Ag}_2(1,3\text{-BDT})]_n$: a. with the six 1,3-benzenedithiolate ligands, b. same as a. with 90° rotation and c. similar to a. with the additional nine 1,3-benzenedithiolate ligands. Blue, cyan, yellow and grey spheres are for Ag1 and Ag3, Ag2 and Ag4, sulfur and carbon atoms, respectively. Hydrogen atoms have been omitted for clarity.

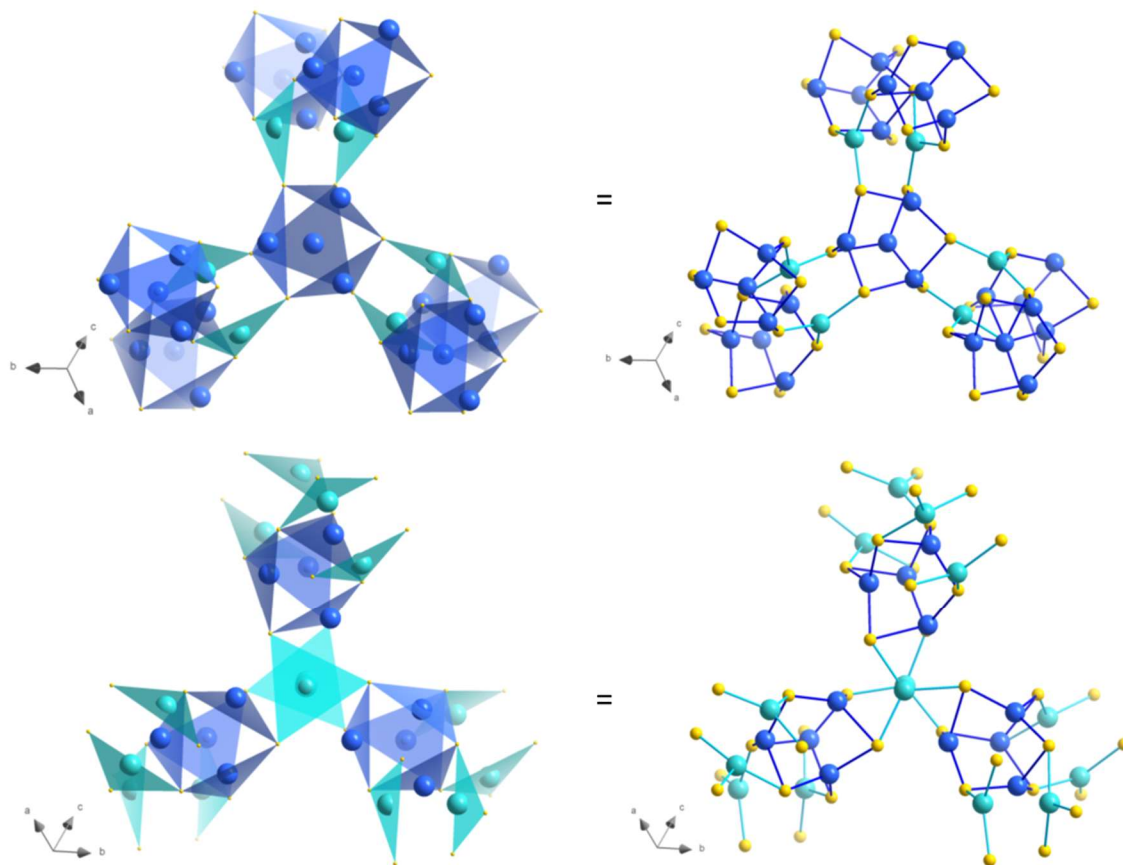


Figure S7. Views of the assemblies of the blue Ag_4S_6 connected to the cyan Ag_2S_6 in $[\text{Ag}_2(1,3\text{-BDT})]_n$. Blue, cyan and yellow spheres are for Ag1 and Ag3, Ag2 and Ag4 and sulfur atoms, respectively. Hydrogen and carbon atoms have been omitted for clarity.

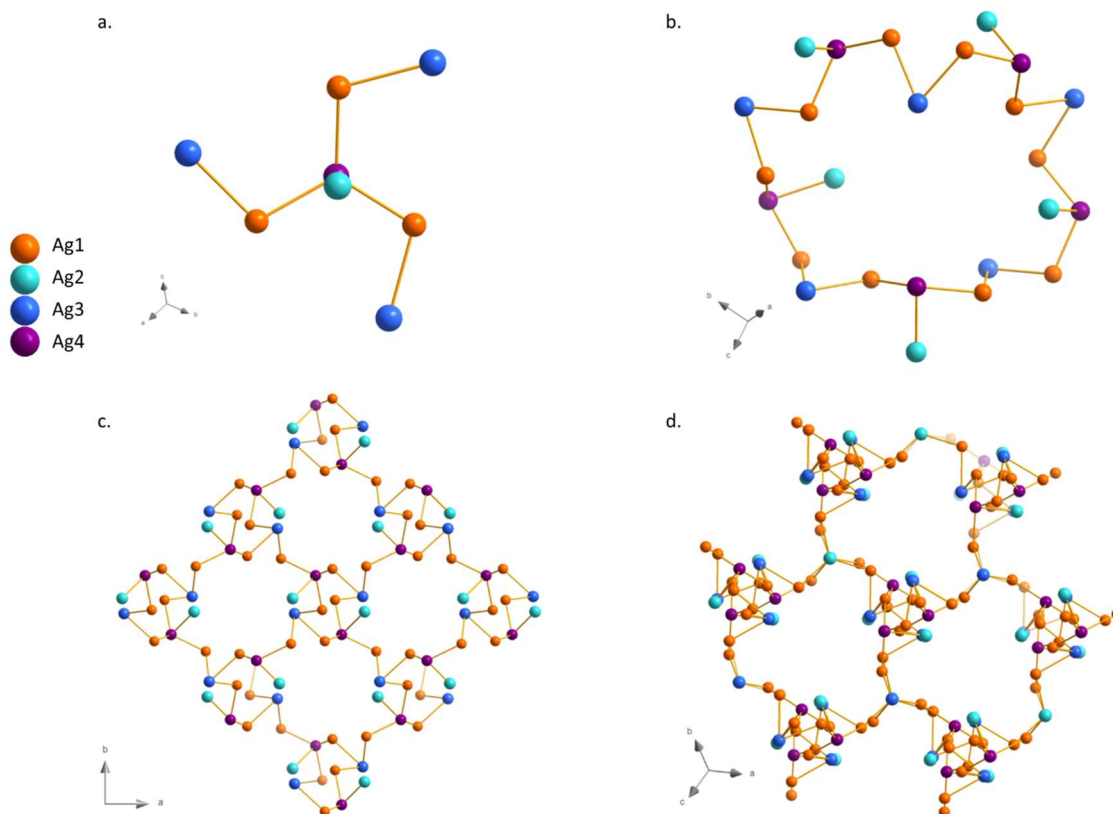


Figure S8. Representations of the four independent silver atoms network in $[Ag_2(1,3-BDT)]_n$. a. Connectivity of the four silver atoms. b. View of the 20-silver atoms cycle (made of Ag1, Ag3 and Ag4) and with the five terminal Ag2 silver atoms. Views of the 3D network along the c axis (c.) and along (111) (d.).

Table S2. Composition in wt% obtained from Rietveld refinements of the *ex situ* PXRD patterns of the $[Ag_2(1,3-BDT)]_n$ samples calcined and/or pressed.

	$[Ag_2(1,3-BDT)]_n$	$\beta-Ag_2S$	Ag	Ag_2SO_4
As-synthesized	100	0	0	0
Calcined 1 h at 200 °C	100	0	0	0
Calcined 1 h at 250 °C	<100	traces	0	0
Calcined 1 h at 300 °C	<100	traces	0	0
Calcined 1 h at 350 °C	68	27	5	0
Calcined 1 h at 450 °C	0	0	58	42
As-synthesized, pressed at 700 MPa	100	0	0	0
Calcined 1 h at 200 °C, pressed at 700 MPa	100	0	0	0
Calcined 1 h at 250 °C, pressed at 700 MPa	<100	traces	0	0
Calcined 1 h at 300 °C, pressed at 700 MPa	<100	traces	0	0
Calcined 1 h at 350 °C, pressed at 700 MPa	54	35	11	0
Calcined 1 h at 350 °C, pressed at 1 GPa	36	57	7	0

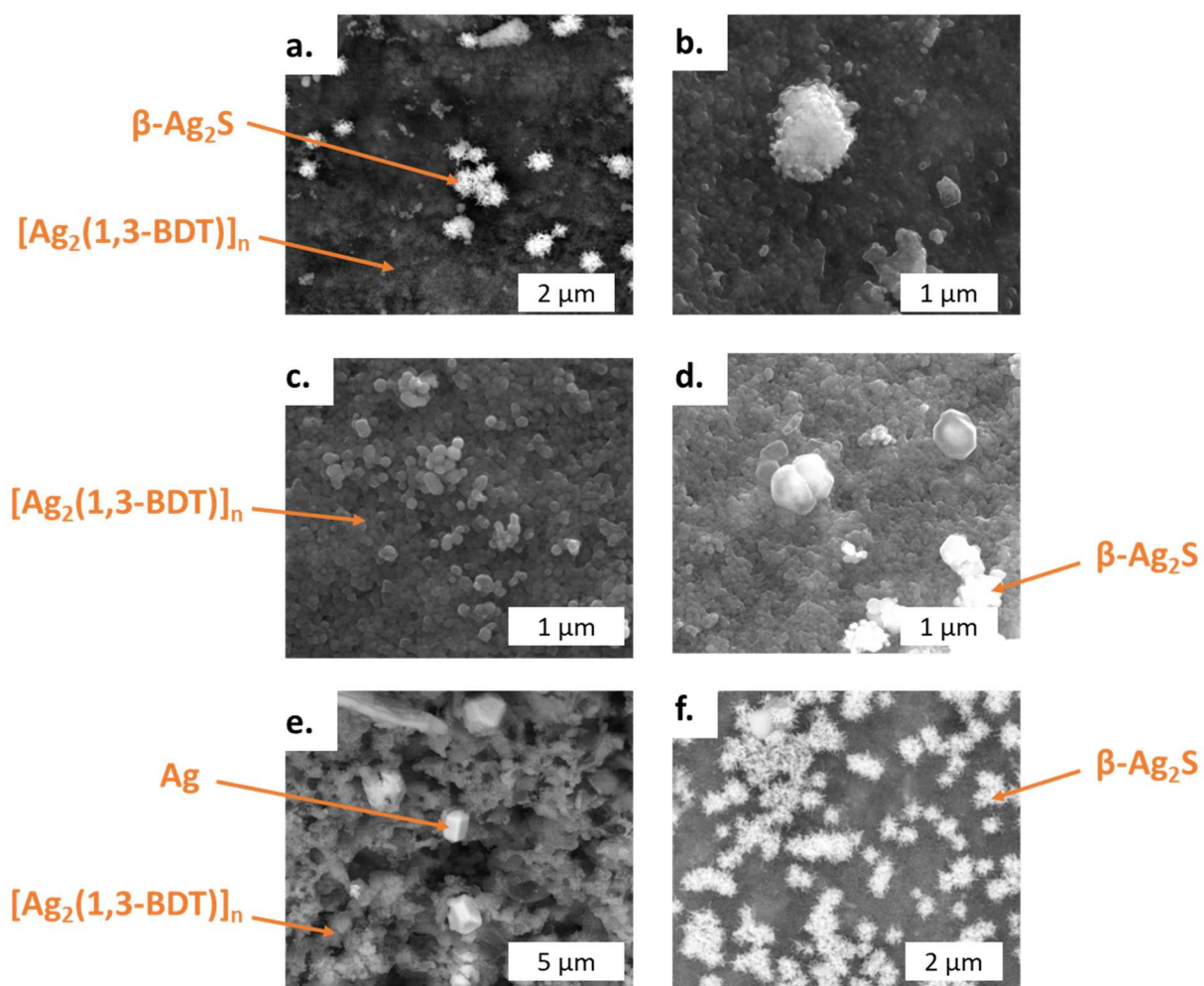


Figure S9. SEM images of $[\text{Ag}_2(1,3\text{-BDT})]_n$ after calcinations for 1 h at 250 (a. and b.), 300 (c. and d.) and 350 °C (e. and f.).

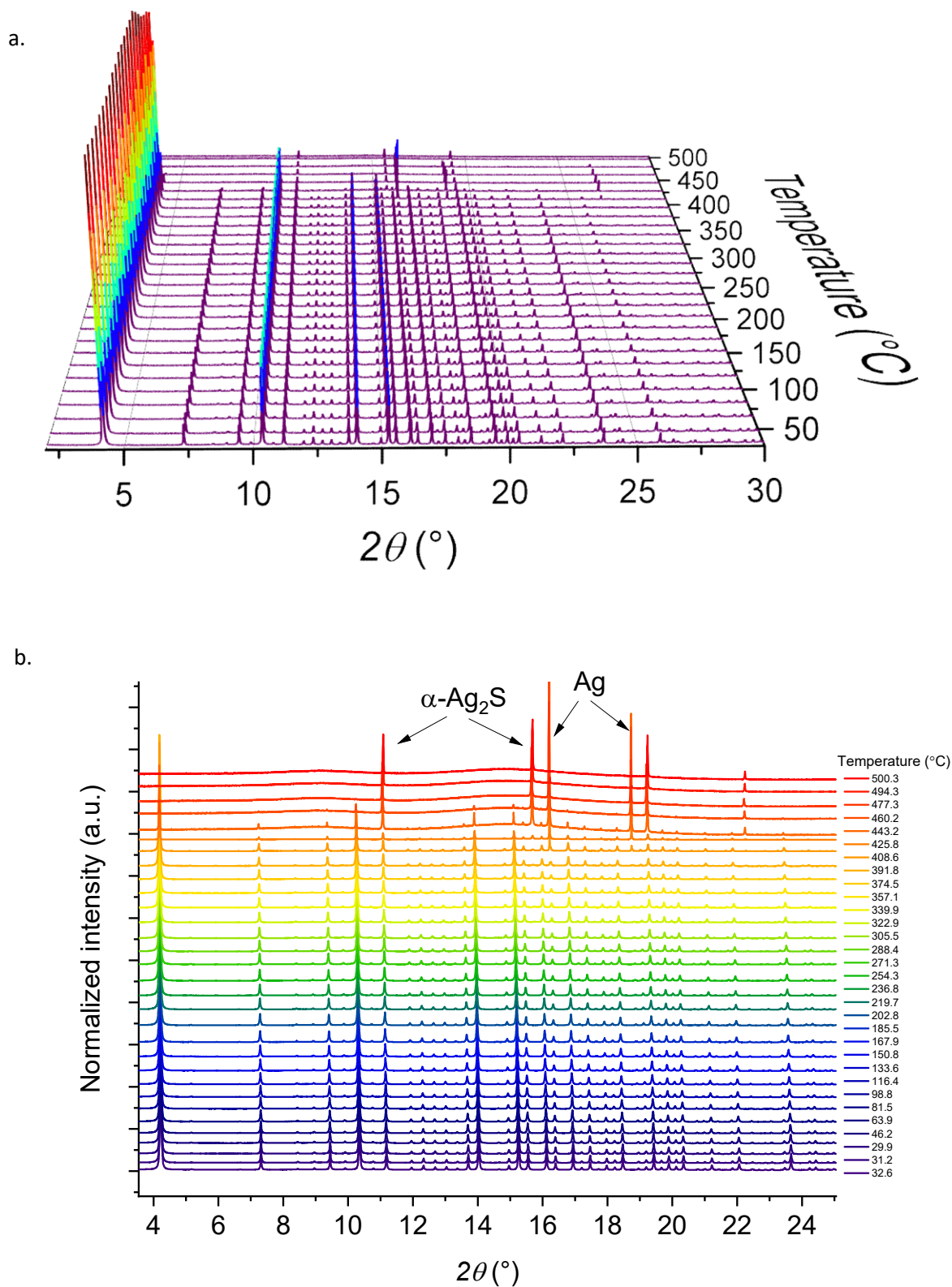


Figure S10. *In situ* PXRD ($\lambda = 0.67122 \text{ \AA}$) patterns of $[Ag_2(1,3-BDT)]_n$ with temperature heat from RT to 500°C at 10°C·min⁻¹ under air: a. by relative intensity and b. by normalized intensity.

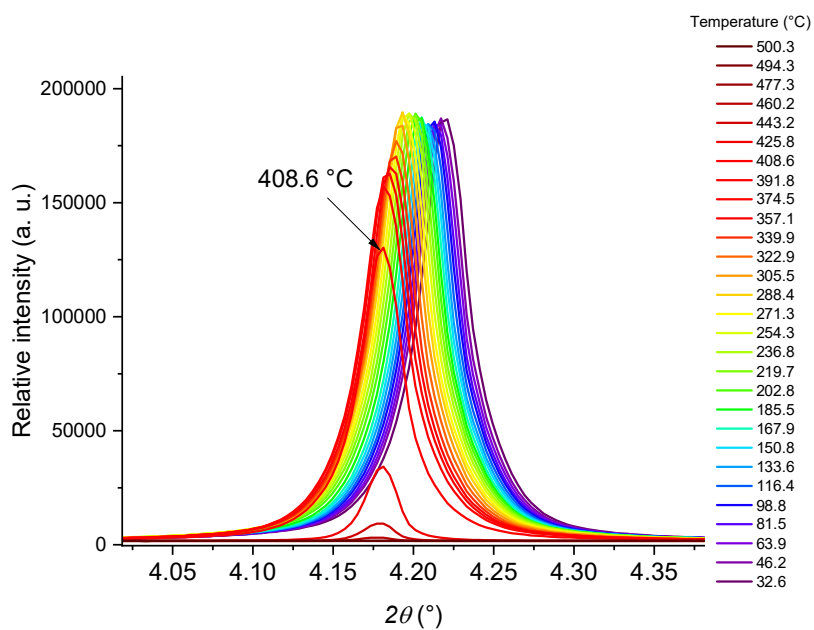


Figure S11. Zoom of the *in situ* PXRD ($\lambda = 0.67122 \text{ \AA}$) of $[\text{Ag}_2(1,3\text{-BDT})]_n$ with temperature heat from RT to 500°C at $10^\circ\text{C}\cdot\text{min}^{-1}$ under air.

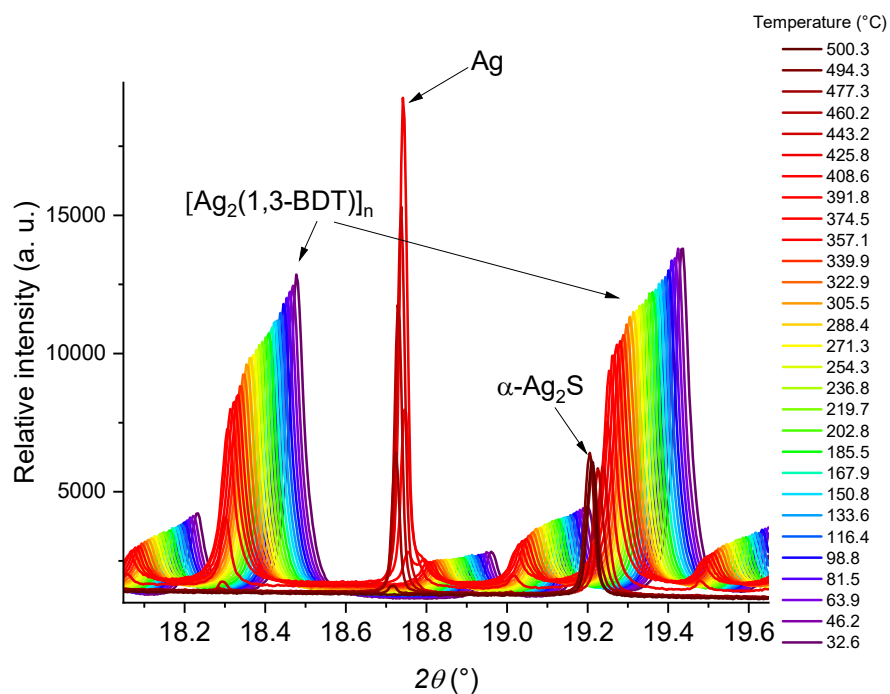


Figure S12. Zoom of the *in situ* PXRD ($\lambda = 0.67122 \text{ \AA}$) of $[\text{Ag}_2(1,3\text{-BDT})]_n$ with temperature heat from RT to 500°C at $10^\circ\text{C}\cdot\text{min}^{-1}$ under air.

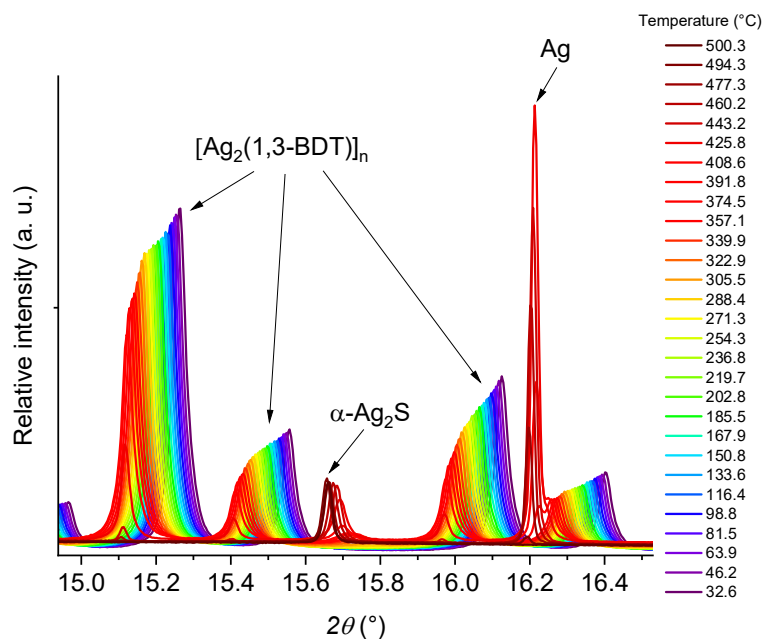


Figure S13. Zoom of the *in situ* PXRD ($\lambda = 0.67122 \text{ \AA}$) of $[\text{Ag}_2(1,3\text{-BDT})]_n$ with temperature heat from RT to 500 °C at $10^\circ\text{C}\cdot\text{min}^{-1}$ under air.

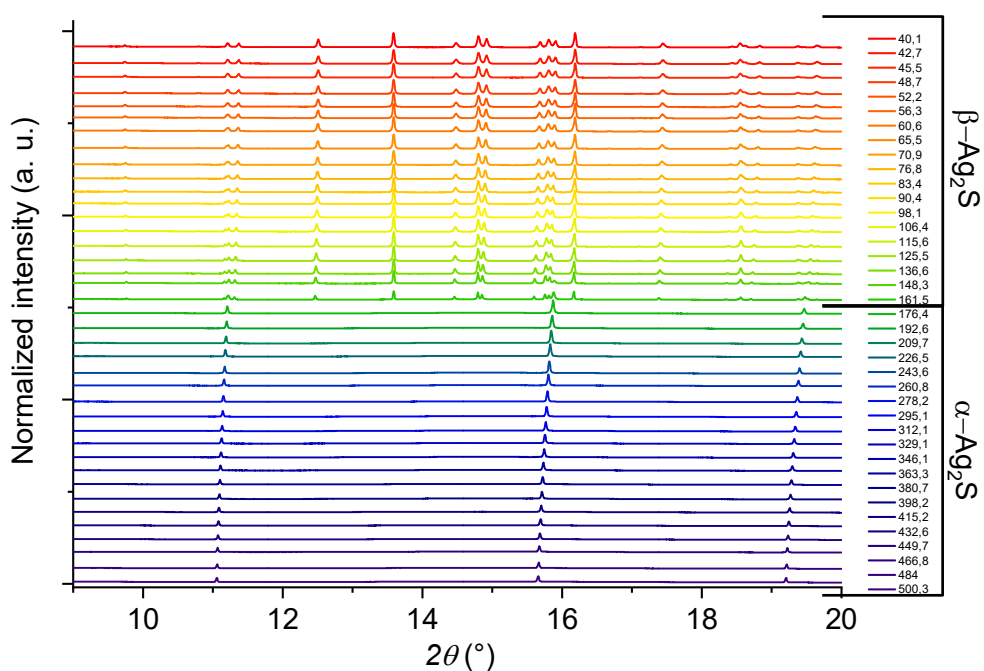


Figure S14. *In situ* PXRD patterns ($\lambda = 0.67122 \text{ \AA}$) of the temperature decreasing from 500 °C to 40 °C. The figure shows the presence of $\alpha\text{-Ag}_2\text{S}$ between 500 °C and 176 °C and its phase change to $\beta\text{-Ag}_2\text{S}$ from 161 °C to 40 °C.

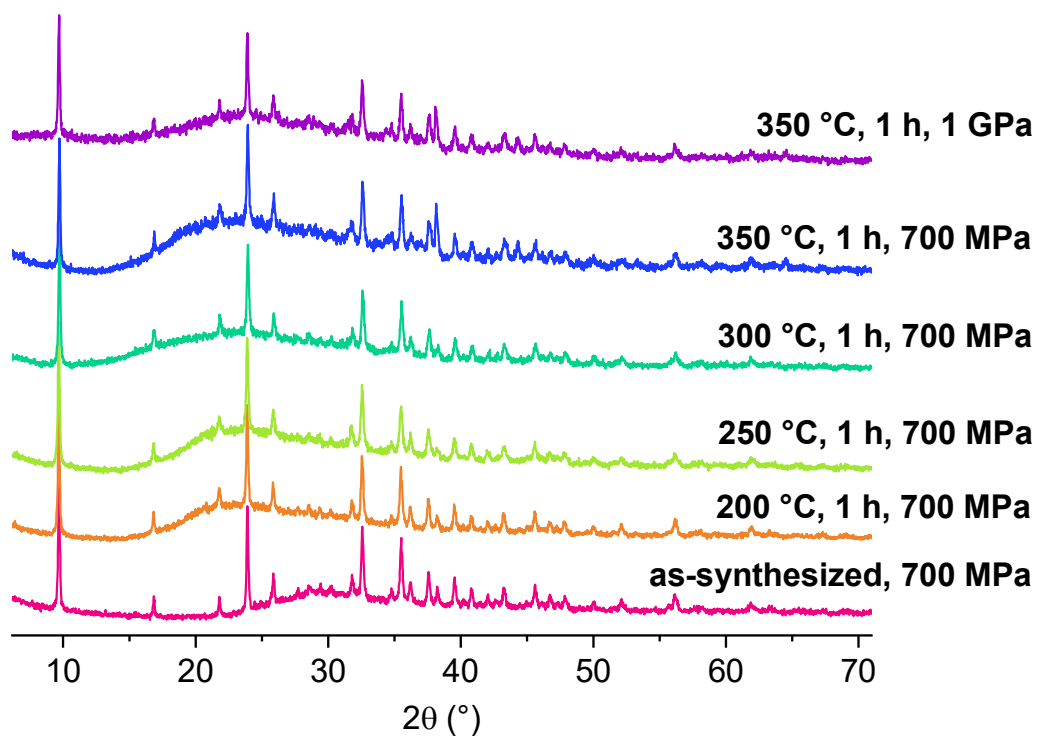


Figure S15. *Ex situ* PXRD patterns ($\lambda = 1.54056 \text{ \AA}$) at RT carried out on pellets, obtained with pressure of 700 MPa or 1 GPa, of $[Ag_2(1,3-BDT)]_n$ as synthesized and calcined for 1 h from 200 to 350 °C. The broad baseline is originating from the different supports used to analyze the 4 mm diameter pellets.

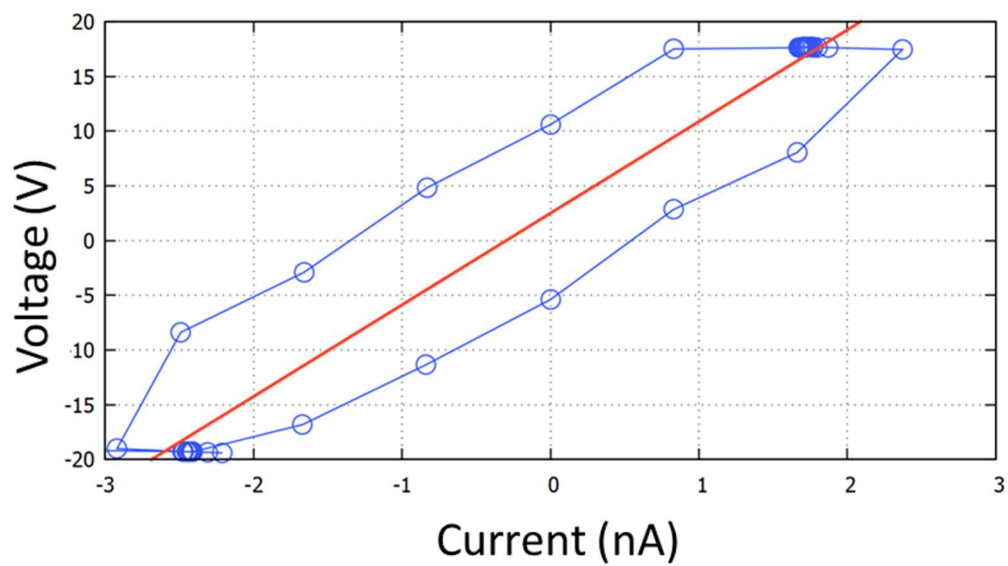


Figure S16. I-V curve of a pellet of the as-synthesized $[(Ag_2(1,3-BDT))_n]_n$ pressed at 1 GPa.

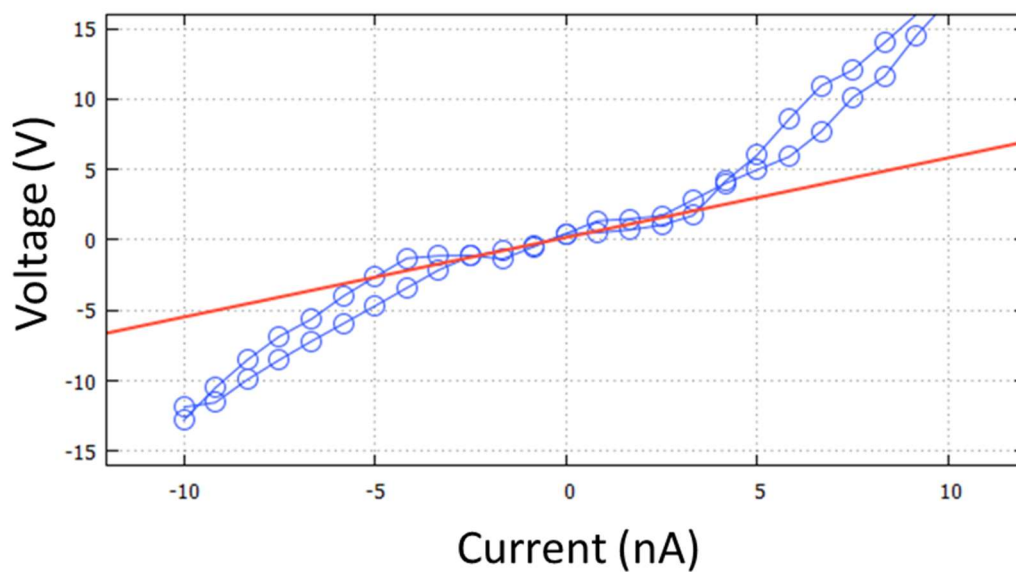


Figure S17. I-V curve of a pellet of the $[(Ag_2(1,3-BDT))_n]_n$ calcined at 300°C and pressed at 1 GPa.

Table S3. Density, current, resistivity and conductivity measures on the pellets pressed at 700 MPa or 1 GPa of $[\text{Ag}_2(1,3\text{-BDT})]_n$ as-synthesized and calcined.

	Pressure	$[\text{Ag}_2(1,3\text{-BDT})]_n$ (wt%)	$\beta\text{-Ag}_2\text{S}$ (wt%)	Ag (wt%)	Measured density ($\text{g}\cdot\text{cm}^{-3}$)	Current (nA)	Resistivity ($\text{G}\Omega$)	Conductivity ($\text{S}\cdot\text{cm}^{-1}$)
As-synthesized	700 MPa	100	0	0	2.61	0.64	27.3	$1.02\cdot 10^{-10}$
As-synthesized	1 GPa	100	0	0	2.81	1.99	20	$1.0\cdot 10^{-10}$
Calcined 1 h at 200 °C	700 MPa	100	0	0	2.80	0.58	25.6	$1.13\cdot 10^{-10}$
Calcined 1 h at 250 °C	700 MPa	<100	traces	0	2.91	1.99	8.64	$3.25\cdot 10^{-9}$
Calcined 1 h at 300 °C	700 MPa	<100	traces	0	3.07	1.99	1.01	$1.43\cdot 10^{-7}$
Calcined 1 h at 300 °C	1 GPa	<100	traces	0	2.86	1.99	0.1	$1.0\cdot 10^{-7}$
Calcined 1 h at 350 °C	700 MPa	54	35	11	2.75	1.99	1.3	$6.4\cdot 10^{-7}$
Calcined 1 h at 350 °C	1 GPa	36	57	7	2.83	1.99	0.88	$1.39\cdot 10^{-7}$
Calcined 1 h at 450 °C	1 GPa	nm	nm	nm	8.38	1000	$2\cdot 10^{-9}$	$7.53\cdot 10^{-5}$

nm: not measured

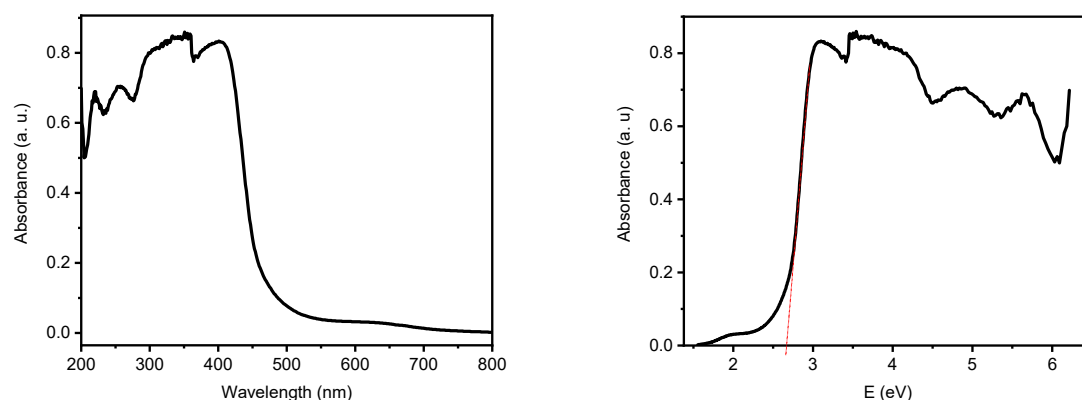


Figure S18. Solid state UV-visible absorption spectrum of $[\text{Ag}_2(1,3\text{-BDT})]_n$.

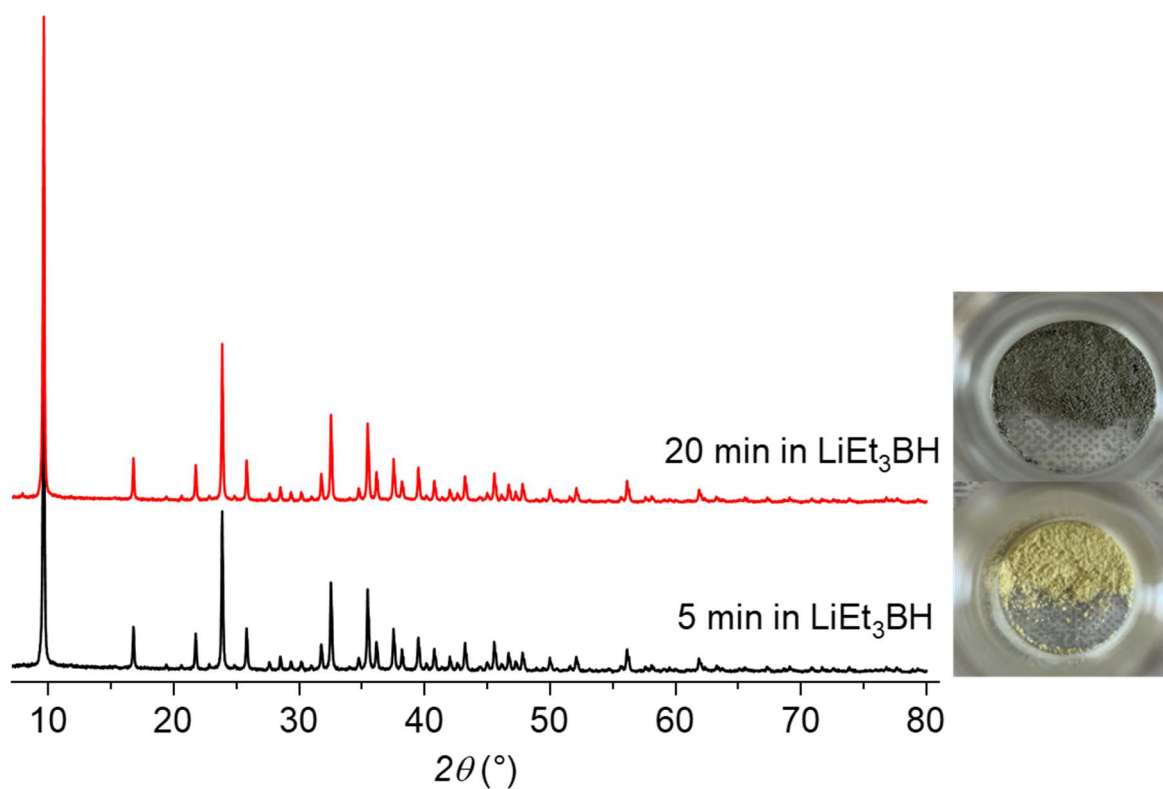


Figure S19. PXRD patterns of $[\text{Ag}_2(1,3\text{-BDT})]_n$ dispersed for 5 (black) and 20 (red) min in LiEt_3BH and the corresponding photo of the powders.

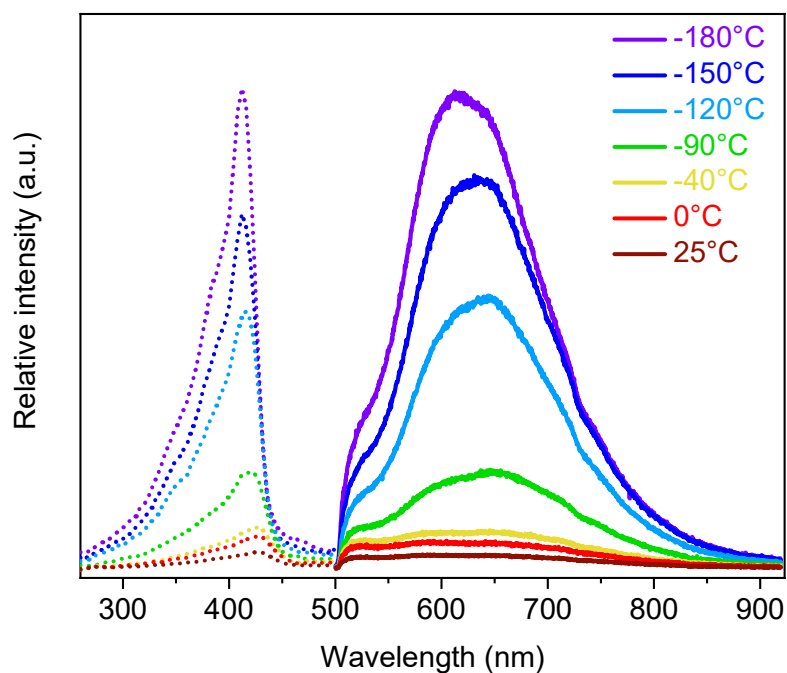


Figure S20. Temperature-dependent solid state excitation ($\lambda_{em} = 600$ nm, dotted lines) and emission ($\lambda_{ex} = 410$ nm, plain lines) spectra of $[Ag_2(1,3-BDT)]_n$.

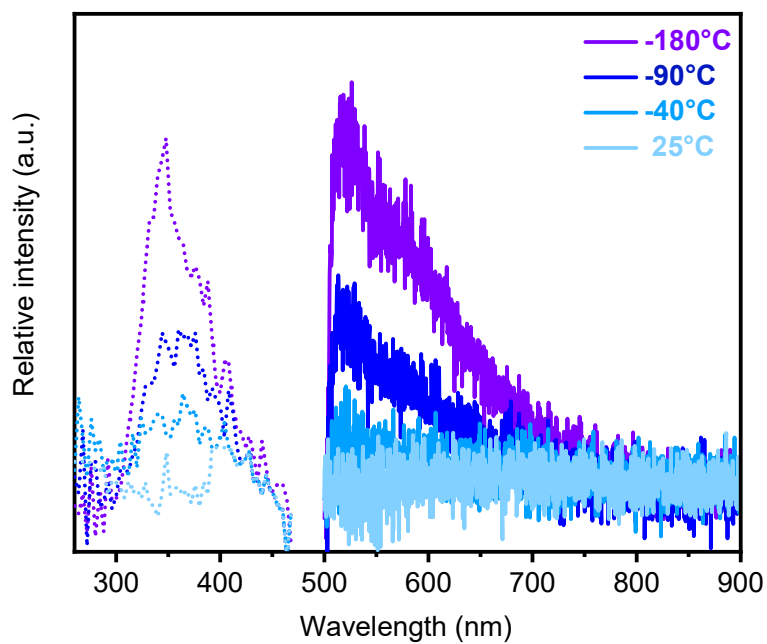


Figure S21. Temperature-dependent solid-state excitation ($\lambda_{em} = 550$ nm, dotted lines) and emission ($\lambda_{ex} = 320$ nm, plain lines) spectra of the free ligand 1,3-H₂BDT.

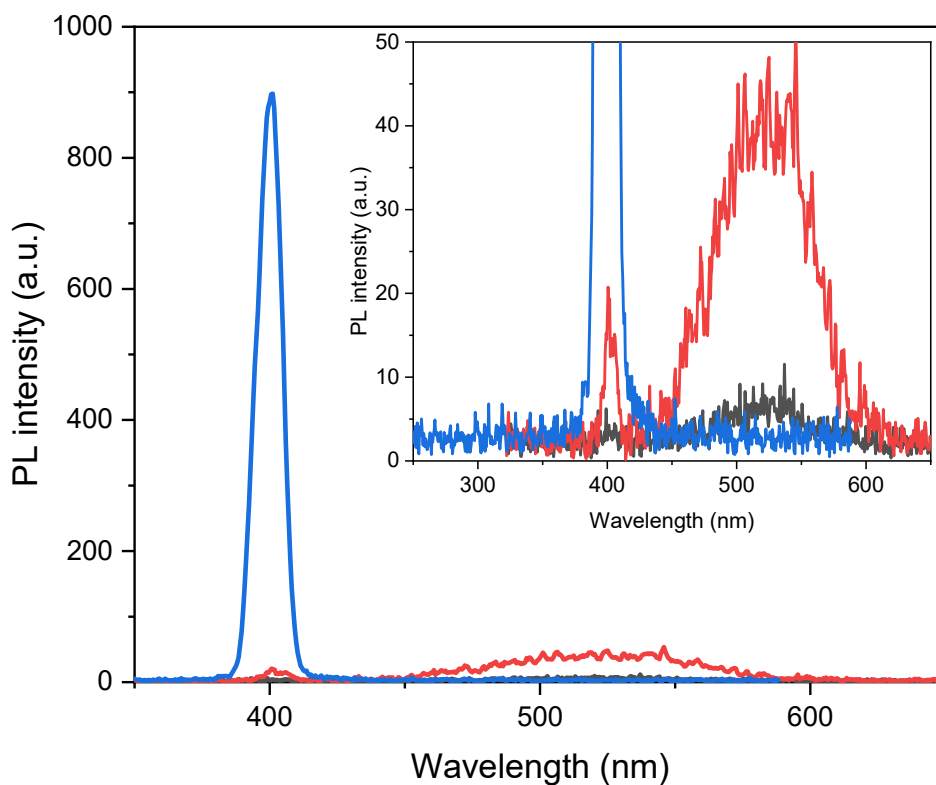


Figure S22. Second Harmonic Generation responses with incident beam at $\lambda = 800$ nm of KDP (blue), $[\text{Ag}_2(1,3\text{-BDT})]_n$ in the same conditions of KDP (black) and with more gain (red). Inset a zoom on the $[\text{Ag}_2(1,3\text{-BDT})]_n$ SHG signals.

- 1 (a) *Topas V5.0: General Profile and Structure Analysis Software for Powder Diffraction Data*, Bruker AXS Ltd, **2014**; (b) A. Altomare; C. Cuocci; C. Giacovazzo; A. Moliterni; R. Rizzi; N. Corriero; A. Falcicchio, *J. Appl. Cryst.*, 2013, **46**, 1231.